Ordered structures in a nonideal dusty glow-discharge plasma

A. M. Lipaev, V. I. Molotkov, A. P. Nefedov,*) O. F. Petrov, V. M. Torchinskiĭ, V. E. Fortov, A. G. Khrapak, and S. A. Khrapak

Scientific Research Center for the Thermal Physics of Pulsed Effects, Russian Academy of Sciences, 127412 Moscow, Russia
(Submitted 5 May 1997)
Zh. Éksp. Teor. Fiz. **112**, 2030–2044 (December 1997)

The formation of ordered structures of charged macroparticles in a constant-current neon glow-discharge plasma is investigated. Experiments were performed with two types of particles: thin-walled glass spheres 50–63 μm in diameter and particles of Al_2O_3, 3–5 μm in diameter. Formation of quasicrystalline structures is observed in the standing strata and in an artificially created double electric layer. The formation of extended filamentary structures of macroparticles in the absence of visible stratification of the positive column has been observed for the first time. The influence of the discharge parameters on the formation of the ordered structures and their melting is examined. The form of the interaction potential between the charged macroparticles is considered, as well as changes in the conditions for maintaining the discharge in the presence of high concentrations of dust particles. © *1997 American Institute of Physics.* [S1063-7761(97)00912-8]

1. INTRODUCTION

The presence of macroscopic particles can have a substantial effect on the properties of a low-temperature plasma. Particles heated to a sufficiently high temperature can, by emitting electrons and acquiring a positive charge, significantly increase the electron concentration in the plasma. A similar effect can occur under conditions in which the dominant process is photoemission or secondary electron emission. Cold particles, on the other hand, absorb electrons from the plasma, acquire a negative charge, and reduce the free electron concentration in the plasma. Charged particles interact with electric and magnetic fields, and the Coulomb interaction between particles can lead to a highly nonideal plasma.

A dusty plasma was first observed under laboratory conditions by Langmuir in the 1920's.[1] However, its active investigation began only in recent decades in connection with a long list of applications such as the electrophysics and electrodynamics of the combustion products of rocket fuels, the electrophysics of the working body of solid-fuel magnetohydrodynamic generators, and the physics of dust clouds in the atmosphere.[2–6] Dust and dusty plasma are widely distributed in the universe. They have been detected in planetary rings, comet tails, and in interplanetary and interstellar clouds.[7–9]

In the last ten years there has been heightened interest in studying the properties of dusty plasmas in connection with the expanded use of the technology of plasma sputtering and etching in microelectronics and in the production of thin films.[10–13] The presence of particles in plasma not only leads to contamination of the surface of the semiconductor element and thereby to an increased yield of defective components, but also perturbs the plasma in a frequently unpredictable way. The reduction or prevention of these negative effects is impossible without an understanding of the processes of formation and growth of condensed particles in a gas-discharge plasma, their transport mechanism, and their influence on the properties of the discharge.

For surface treatment, low-pressure radio-frequency gas-discharge plasma is usually used.[14] The degree of ionization of such a plasma is low ($\sim 10^{-7}$), the electron energy is a few eV, and the ion energy is near the thermal energy of the atoms (≈ 0.03 eV). A neutral, nonemitting particle incident on such a plasma is buffeted by fluxes of all the particles present in the plasma, including electrons and ions. It is customary to assume that electrons incident on the surface of the particle are absorbed, and the ions raining down upon its surface knock out electrons and recombine with them.

As a consequence of the great difference in masses and temperatures of the electrons and ions, the electron flux exceeds the ion flux by several orders of magnitude, and the particle acquires a negative charge. The negative electrostatic potential on the particle leads to repulsion of electrons and attraction of ions. The charge of the particle changes until the electron and ion fluxes on the particle equalize.

The steady-state charge Z or floating potential φ_p can be estimated within the framework of the orbital motion model, widely used in the theory of plasma probes.[15] This model is valid in the collisionless regime for particles of sufficiently small dimensions

$$R_p \ll \lambda \ll l, \tag{1}$$

where R_p is the particle radius, and λ and l are the typical screening length and the typical mean free path of the electrons or ions, whichever is the smaller. Balance of electron and ion currents leads to the following equation for φ_p:

$$N_e \sqrt{\frac{T_e}{m_e}} \exp\left(\frac{e\varphi_p}{T_e}\right) = N_i \sqrt{\frac{T_i}{m_i}} \exp\left(1 - \frac{e\varphi_p}{T_i}\right), \tag{2}$$

where $T_{e(i)}$ and $m_{e(i)}$ are the temperature and mass of the electrons (ions).

Equation (2) enables one to estimate the potential and charge of an isolated particle in the plasma. The typical charge of a micron-sized particle lies within the range from 10^3 to 10^5 electron charges. The walls of the discharge

chamber and the electrodes acquire a negative potential. All this makes it possible under certain conditions to compensate for the effect of gravitation, and leads to levitation of the particles above the lower electrode or floor of the discharge chamber. Methods for confining a dusty plasma in special traps, which make it possible to reduce contamination of the work surfaces, are based on this effect.

The thermodynamic properties of dusty plasmas are mainly determined by the magnitude of the nonideality parameter Γ, which is equal to the ratio of the Coulomb potential energy to the kinetic energy of thermal motion characterized by the particle temperature T_p:

$$\Gamma = \frac{Z^2 e^2}{a T_p}, \quad a = \left(\frac{3}{4\pi N_p} \right)^{1/3}, \tag{3}$$

where a is the mean distance between particles, and N_p is their concentration. Thanks to the large charge of the particles, nonideality in the interaction between particles can enter significantly earlier than nonideality of the electron–ion subsystem, despite the fact that the particle concentration is usually low in comparison with the electron and ion concentrations.

From the simplest and most widely studied model of a one-component plasma it is well known that for $\Gamma > 1$ short-range order appears in the system, and for $\Gamma \approx 170$ a one-component plasma crystallizes.[16] The one-component model cannot claim to provide a faithful description of the properties of a dusty plasma, above all because it neglects screening effects. Nevertheless, a number of papers, on the basis of qualitative results of the one-component model, express the view that near-range order is possible in a thermal-equilibrium dusty plasma, and even crystallization.[4,5,17]

Recently, ordered structures of dust particles were detected in a thermal plasma at atmospheric pressure at a temperature of around 1700 K (Refs. 18 and 19). Similar considerations led Ikezi[20] to infer the possibility of crystallization of a dust subsystem in a nonequilibrium gas-discharge plasma. Eight years after the publication of this paper, a dust crystal was finally observed experimentally in a high-frequency discharge near the lower electrode at the boundary of the near-cathode region,[21–24] and later in the strata of a stationary glow-discharge.[25,26]

A plasma crystal can have varied crystal structure, with a lattice constant on the order of fractions of a millimeter, which makes it possible to observe it practically with the naked eye. Plasma crystals possess a great many virtues, making them an indispensable instrument both in the study of highly nonideal plasmas and in the study of the fundamental properties of crystals. These include, first and foremost, simplicity of preparation, observation, and parameter control, and their short equilibrium relaxation times and response times to external perturbations.

A dust crystal is not a unique example of the appearance of long-range order in Coulomb systems. In his time, Wigner showed[27] that upon cooling, an electron gas can condense and form an ordered crystalline structure, the so-called ''Wigner crystal.'' Recently, crystallization of a quantum electron liquid with formation of a Wigner crystal was investigated experimentally.[28] Crystal structures, also in one-component systems, were observed in electrostatic vacuum traps on charged macroparticles[29] and in Paul and Penning traps on Mg or Be ions cooled to very low temperatures ($\sim 10^{-3}$ K).[30–32] A Coulomb crystal is also realized in colloidal suspensions.[33] Colloidal crystals consist of almost monodisperse micron-sized particles suspended in an electrolyte, where they become charged to $Z = -(10^3 - 10^4)$ and are screened by ions of both signs in the electrolyte. According to a conjecture of Deryagin and Landau,[34] under certain conditions the Coulomb interaction between the particles makes formation of a crystal structure energetically more favorable. Strong coupling between particles takes place at distances less than the screening radius, which in colloidal suspensions is very small. This leads to the result that for crystallization a rather high particle density ($N_p \sim 10^{12}$ cm^{-3}) is necessary. As a consequence, colloidal crystals are usually opaque, hindering experimental study of their bulk properties. To the drawbacks of colloidal crystals as an instrument of physical study may also be added their long equilibrium relaxation time, amounting to several weeks.

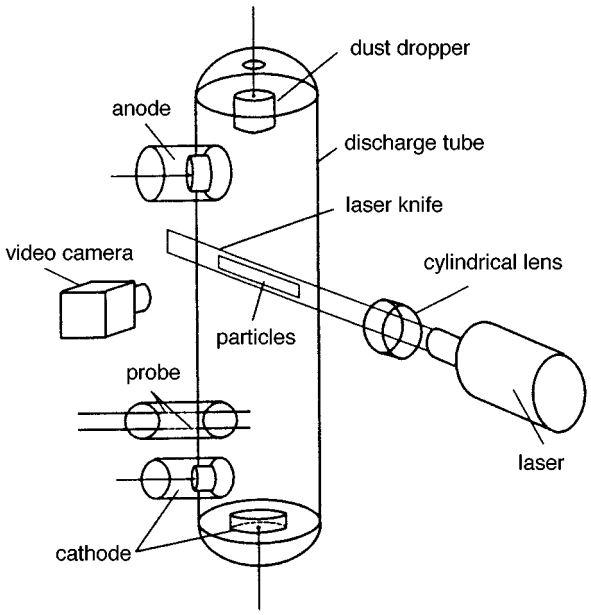

FIG. 1. Schematic of the experimental setup.

The present paper investigates the formation of ordered structures of charged macroparticles of various sizes in a constant-current glow-discharge plasma in neon. The influence of the discharge parameters on the possibility of the existence of quasicrystalline structures of dust particles is examined, along with the conditions for their formation and destruction. We consider the question of the form of the interaction potential between the macroparticles, and also the effect of the macroparticles themselves on the conditions for maintaining the discharge.

2. EXPERIMENTAL SETUP

A glow-discharge was created in neon in a cylindrical, vertically positioned tube with cold electrodes. A schematic of the setup is shown in Fig. 1. The inner diameter of the

tube was 3 cm, the length of the tube was 60 cm, the distance between the electrodes situated in lateral nibs of the tube was 40 cm. A double mobile probe was also placed in the tube. The discharge current was varied within the range from 0.1 to 10 mA, and the neon pressure, from 0.2 to 2 Torr. Discharge regimes with standing strata existed in this range.

Micron-sized particles to be introduced into the plasma were held in a cylindrical container located in the upper part of the gas-discharge tube. The bottom of the container was fashioned from a metal mesh with a spacing of 100 μm. When the container was shaken, particles rained down into the positive column of the discharge. The particles were visualized with the aid of illumination in either the horizontal or vertical planes by a probe laser beam. The beam from an argon laser was formed by a cylindrical lens into a planar converging beam with thickness of the beam waist at the center of the discharge tube equal to 150 μm and width 40 mm.

The horizontal probe beam could be vertically translated along the length of the tube, and the vertical probe beam, both in height and radius. Light scattered by the particles was observed with the aid of a CCD camera at an angle of 60° in the case of the horizontal beam and at an angle of 90° in the case of the vertical beam. The output signal of the camera was recorded on video tape. Note that individual particles and the cloud of particles as a whole are visible in the laser light even to the naked eye.

Oscillations of the discharge connected with repositioning of the cathode spot are observed in a glow-discharge with a cold cathode, which causes fluctuations of the ordered structures. To damp these oscillations, an additional tube with a constriction was introduced. This inset was positioned in the lower part of the discharge tube above the cathode.

3. EXPERIMENTAL RESULTS AND DISCUSSION

3.1. Formation of ordered structures in strata of the positive column

In the experiments we used two types of particles: particles of borosilicate glass ($\rho = 2.3$ g/cm^3) in the form of thin-walled, hollow spheres (microballoons) of diameter 50–63 μm with wall thickness 1–5 μm (the mass of the particles M_p lies in the range from 2×10^{-8} to 10^{-7} g) and Al_2O_3 particles ($\rho = 4$ g/cm^3) with diameter 3–5 μm (M_p lies in the range from 6×10^{-11} to 3×10^{-10} g).

In the presence of standing strata in the positive column of the discharge, dust particles that poured down from the container hovered in the form of a cloud in the center of the luminous part of the stratum. The charged microscopic particles captured into the stratum formed ordered quasicrystalline structures, whose size and shape depended on the discharge parameters. The region of existence of the strata for the given discharge tube lies in the range of neon pressures from 0.1 to 1.7 Torr for the discharge current varying from 0.1 to 10 mA. The length of the luminous part of the stratum was 10 mm at a pressure $p = 1.2$ Torr and grew to 25 mm at $p = 0.2$ Torr. The distance between the luminous parts of the strata depended weakly on the discharge parameters and lay within the limits 35–50 mm. Note that the ordered structures of charged particles formed in the strata have a narrower existence region.

The formation process proceeds as follows: after being shaken out of the container, the particles fall past their equilibrium position and then, over the course of several seconds, rise back up and form into an ordered structure which is preserved for as long as desired provided the discharge parameters are left unchanged. Individual particles can move upward toward the anode and along the periphery of the stratum. In addition, peculiar orbital motions of the particles around the ordered structures are observed. Contrary circular motions of individual particles are also observed. A particle completes one revolution in approximately 10 s.

The simultaneous existence of ordered structures in several neighboring strata was observed. By way of example, Fig. 2a shows an image of structures of charged microballoons of borosilicate glass in two neighboring strata. By varying the discharge parameters (current, pressure) it is possible to obtain coalescence of the structures in neighboring strata into one long, extended formation. Figure 2b displays such a structure.

Figure 3 shows digitized images of structures of Al_2O_3 particles taken in the horizontal plane for two values of the discharge current I_p: 0.4 and 3.9 mA for neon pressure $p = 0.3$ Torr. Figure 4 shows two plots of the conditional particle distribution function $n(r) = n_2(r)/n_1(r)$, obtained by processing the corresponding images in Fig. 3; n_1 and n_2 are the corresponding unary and binary functions.[35,36] The function $n(r)$ is the particle number density at a distance r from some particle. The choice of this function instead of the commonly used pairwise correlation function $g(r)$ is dictated by the inhomogeneity of the investigated structures associated with their relatively small dimensions.

Figure 4 plots the distribution function $n(r)$ for each of the above two discharge regimes for the central part of a horizontal cross section of the structure, and for all of the particles in the given cross section (the central part of the horizontal cross section in our case consists of the particles lying inside a circle whose center coincides with the center of mass of the cross section, and includes around 40% of all the particles observed in the cross section). It can be seen that for $I_p = 0.4$ mA at least three maxima of $n(r)$ can be identified, which suggests the existence of long-range order in the investigated dusty plasma. This corresponds to a crystal-like structure.

It follows from these images and distribution functions that with increasing discharge current there is a tendency toward the destruction of long-range order (''melting''), and at $I_p = 3.9$ mA only short-range order is observed.

Note that the destruction of long-range order accompanying an increase in the discharge current above all entrains the periphery of the structure. The central part of the formation preserves its former order. In addition, with increasing I_p, spontaneous oscillations of individual macroparticles are observed. In this situation, such particles move along circular trajectories whose radii increase with distance from the center of the structure. Circular oscillations of the particles were also observed in a dusty rf discharge plasma when the gas pressure was decreased.[37] As can be seen from Fig. 4, de-

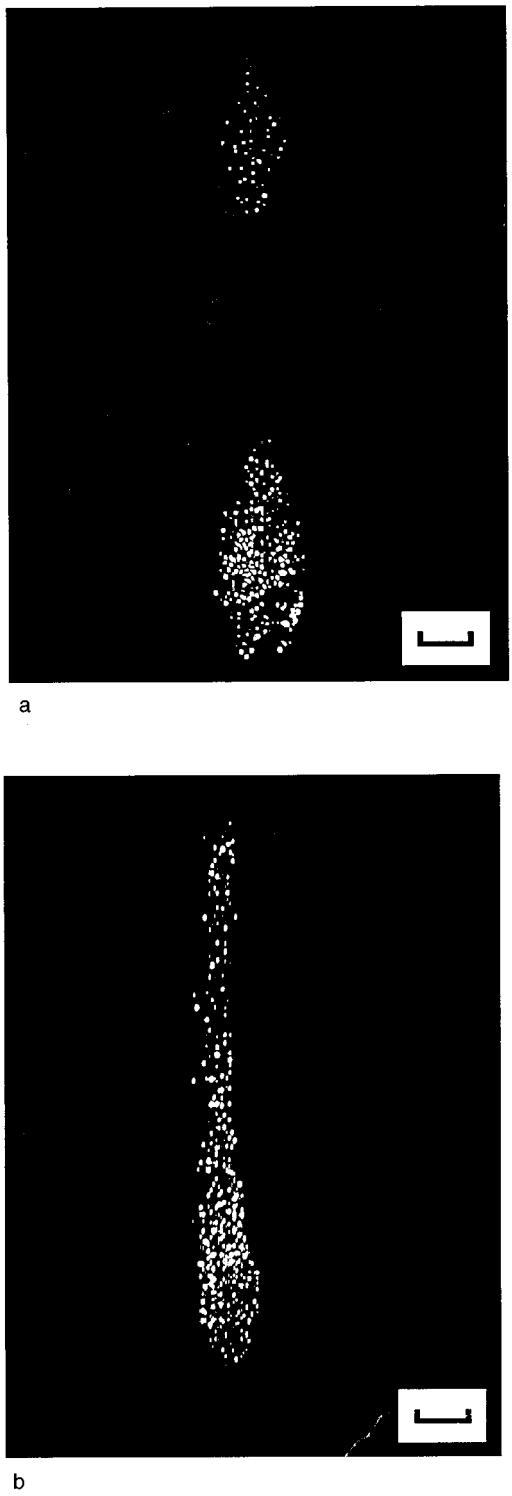

FIG. 2. Video images of structures of charged microballoons of borosilicate glass: a) in two neighboring strata ($p=0.5$ Torr, $I_p=0.5$ mA), b) after their coalescence ($p=0.4$ Torr, $I_p=0.4$ mA). The scale in the figure corresponds to 3 mm.

spite varying I_p by an order of magnitude, the mean interparticle distance a, equal to 250 μm, remains essentially unchanged.

At a higher neon pressure of 0.7 Torr, less ordered structures of charged Al_2O_3 particles are observed in the range of currents from 0.7 to 7 mA. The interparticle distance a in this case is also independent of the discharge current and is equal to 280 μm.

The constancy of the interparticle distance a in the face of a significant change in the discharge current and, consequently, the electron concentration N_e, differs sharply from the appreciable dependence of a on the power fed to the rf discharge (and accordingly on the electron concentration N_e) observed in Ref. 23.

Figure 5 shows a digitized image of the structure of charged microballoons of borosilicate glass in one of the vertical planes. Figure 6 plots the corresponding distribution functions for the central part of the structure and the structure as a whole. These results demonstrate the existence of significant ordering of the particles in the vertical cross sections.

Our experiments revealed the emergence of unusual formations of charged macroparticles: in different discharge regimes, with the disappearance of visible standing strata extended filamentary structures are formed, extending upward from the dark cathode space through the height of the tube. The length of these structures reached 60 mm. Fragments of the filamentary structure are shown in Fig. 7. Near the dark cathode space the number of filaments reaches 7–8, while in the upper part their number is reduced to 1–2. The number of particles per filament (chain) reaches 100–120. Note that the extended filamentary structures are observed for both types of microscopic particles used in the experiments.

Strata in low-pressure discharges have been experimentally investigated in considerable detail.[38–41] In the positive column of the discharge under the conditions of interest, loss of electron energy in elastic collisions is negligibly small and the electron distribution function is formed under the action of the electric field and the inelastic collisions. This can lead to the appearance of strata—a spatial periodicity of the plasma parameters with characteristic scale $\lambda_1=\varepsilon_1/eE_0\approx 4-5$ cm (ε_1 is the first excitation potential, equal to 16.6 eV for neon, and E_0 is the electric field averaged over the length of the stratum).

The electron concentration, their energy distribution, and the electric field are highly irregular along the length of the stratum. The electric field E is relatively strong at the head of the stratum (around 10–15 V/cm at its maximum)—a region occupying 25–30% of the length of the stratum, and weak (around 1 V/cm) outside this region. The maximum value of the electron concentration is displaced relative to the maximum of E in the direction of the anode.[39] The electron energy distribution is substantially bimodal,[39] and the head of the stratum is dominated by the second maximum, whose center lies near the excitation potential ε_1.

Due to the high floating potential of the walls of the discharge tube, the strata have a substantially two-dimensional character: the center–wall potential difference at the head of the stratum reaches 20–30 V, and the change in the potential takes place in a narrow near-wall layer of thickness 2–3 mm (Refs. 40–42). Thus, an electrostatic trap is found at the head of each stratum, which in the case of vertical orientation is capable of confining particles with high enough charge and low enough mass.

The experimental information above was obtained only

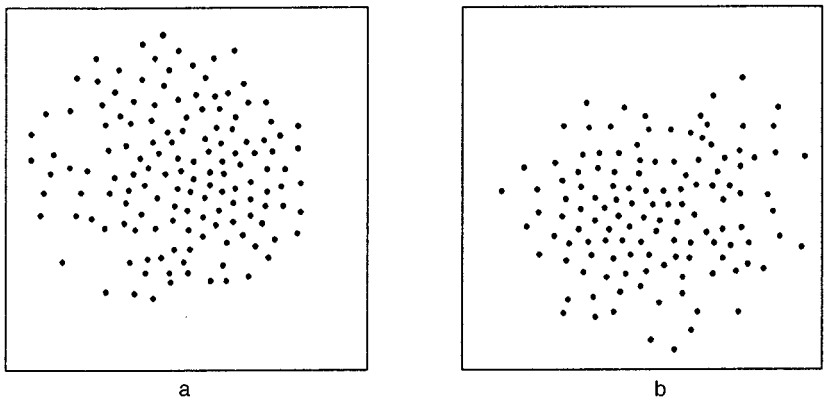

FIG. 3. Digitized video images of structures of Al_2O_3 particles in the horizontal plane for $p=0.5$ Torr: a) $I_p=0.4$ mA, b) $I_p=3.9$ mA. Frame dimensions 5×5 mm^2.

for moving strata; however, there is every reason to believe that for the same discharge parameters, the properties of resting and moving strata are similar.[43] By virtue of the substantially two-dimensional nature of the problem, a theoretical description of the strata in a low-pressure discharge is quite complicated, and at present can lay claim to only a qualitative explanation of the observed effects.[44,42] As a consequence of particles sticking to the probe, efforts under taken in the present work to measure plasma parameters with the aid of a double probe in the presence of macroparticles have not been crowned with success. Nevertheless, the electric field strengths measured in the positive column in a neon discharge in the absence of stratification are in good agreement with the published data. Therefore, in our analysis we will be forced to rely, above all, on the results of an experimental study of strata[40–42] carried out under conditions similar to ours.

The potential of the particle φ_p, and consequently its charge Z, can be estimated with the help of Eq. (2). However, it must be recalled that its derivation employs the Maxwellian electron energy distribution far from the particle. As we have already pointed out, the electron distribution function is bimodal in the strata, and Eq. (2) can be used for estimates only in those regions of the stratum where one of the maxima predominates. Thus, in the region of maximum luminosity, the second maximum, which has energy $T_e\approx\varepsilon_1$, predominates. This makes it possible with the aid of Eq. (2) to estimate the maximum value of the floating potential $\varphi_p\approx-1.65\varepsilon_1\approx-27$ eV. The relation between the potential of a particle and its charge in the linear Debye screening approximation is[45]

$$Z=\varphi_p R_p(1+R_p/\lambda_L), \tag{4}$$

where λ_L is the linearized screening length

$$\lambda_L=\left[4\pi e^2\left(\frac{N_e}{T_e}+\frac{N_i}{T_i}\right)\right]^{-1/2}. \tag{5}$$

This yields a charge $Z\approx-3\times10^4$ for the Al_2O_3 particles, and $Z\approx-7\times10^5$ for the glass particles.

Levitation of macroscopic particles takes place in the region of the stratum where the electrostatic force ZeE is balanced by the gravitational force M_pg. Thus, it is possible to determine the magnitude of the electrostatic field E_m in which particle levitation is possible:

$$E_m=\frac{M_pg}{Ze}. \tag{6}$$

This yields $E_m\approx1$ V/cm for the Al_2O_3 particles and $E_m\approx45$ V/cm for the glass particles. The latter is 3–4 times the fields usually observed at the head of the stratum. However, this disagreement can be partly explained by the separation of particles according to wall thickness, and consequently mass, where this separation takes place directly in

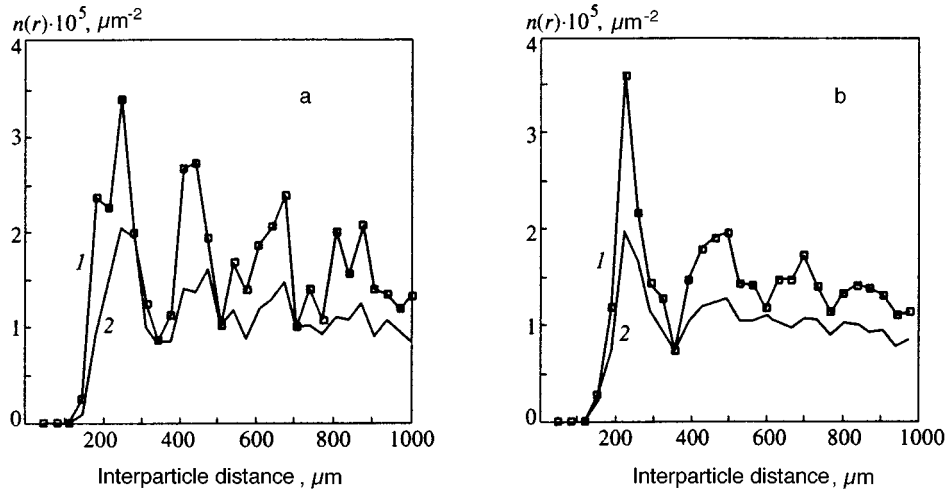

FIG. 4. Distribution functions $n(r)$ for the structures shown in Fig. 3: a) $I_p=0.4$ mA, b) $I_p=3.9$ mA. *1*—$n(r)$ for the central region of the cross section, *2*—for the entire cross section.

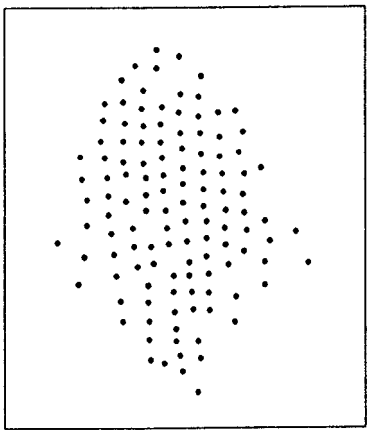

FIG. 5. Digitized video images of structures of charged microballoons of borosilicate glass in the vertical plane for $p=0.2$ Torr and $I_p=0.7$ mA. Frame dimensions 6×7.5 mm^2.

the discharge: particles with minimal M_p/Z are captured, above all the thin-walled ones with wall thickness 1–2 μm. In addition, the very presence of charged particles can lead to an increase in the electric field.

The Coulomb interaction between charged particles is proportional to the product of their charges. Therefore, a large value of Z leads to a strong Coulomb repulsion between particles, and consequently nonideality of the system. For a mean interparticle distance $a=300$ μm at $T=300$ K, the nonideality parameter $\Gamma\sim10^6$ and 10^8 for particles of radius 1.5 and 25 μm, respectively. Note, however, that the particles are screened by the electrons and ions of the plasma, whose concentration varies severalfold along the length of the stratum and lies within the limits $5\times10^7-5\times10^8$ cm^{-3} (Refs. 40–42). The floating potential of the particles is equal in order of magnitude to the electron energy, and significantly exceeds the ion energy. Therefore the screening of the particles is substantially nonlinear. In addition, electron and ion recombination takes place on the surface of the particles, as a result of which there is no reverse charged-particle flux near the particles, and their distribution function is non-Maxwellian. Thus, even the asymptotic behavior of the potential far from the particle surface ceases to be Debye-like, and depends on the distance according to a power law, $\varphi(r)\approx-ZR_P/2r^2$. This effect has long been known, and has been well studied in the theory of spherical electrostatic probes.[15]

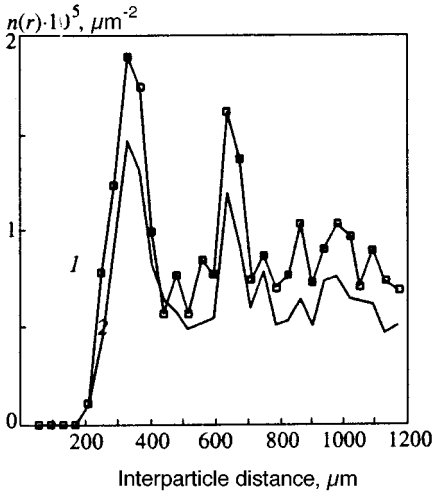

FIG. 6. Distribution functions $n(r)$ for the structure imaged in Fig. 5: *1*—$n(r)$ for the central region of the cross section, *2*—for the entire cross section.

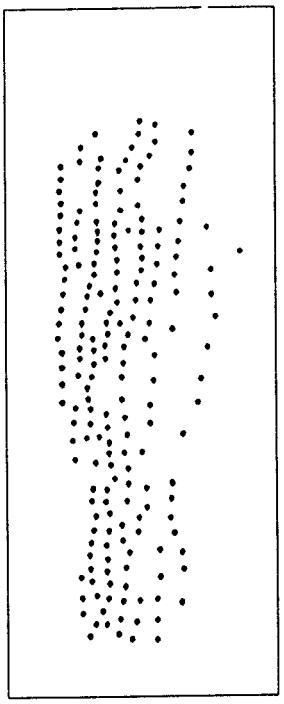

FIG. 7. Digitized video image of a fragment of a filamentary extended structure of charged glass microballoons in the vertical plane for $p=0.4$ Torr and $I_p=0.4$ mA. Frame dimensions 7.5×18 mm^2.

The structure of the screening cloud in the collisionless regime with allowance for the nonlinearity of the Poisson equation and the non-Maxwellian character of the electron and ion energy distribution functions was calculated in Ref. 46 for spherical particles in a helium discharge. It turns out that at small distances the particle potential can be approximated to high accuracy by the Debye–Hückel potential

$$\varphi(r)=\varphi_p\,\frac{R_p}{r}\,\exp\left(-\frac{r-R_p}{\lambda}\right). \tag{7}$$

However $\lambda=\lambda_L$ only in the case of sufficiently small particles ($R_p\ll\lambda_L$), and for large R_p the screening length increases with R_p, reaching and even exceeding the electron screening length $\lambda_e=\sqrt{T_e/4\pi e^2N_e}$.

Figure 8 plots the results of a calculation of $\varphi(r)$ that we performed for a neon discharge, for particles of two sizes, under conditions typical of the mid-region of the strata in neon, and allowing for the non-Maxwellian character of the electron and ion distribution functions due to their absorption by the surface of the macroparticle. It can be seen that the approach to the non-Debye-like dependence $\varphi(r)\propto-1/r^2$ takes place earlier for larger particles, and at distances close to the mean interatomic distance in the levitating ordered structures. This effect can lead to an increase in repulsion at

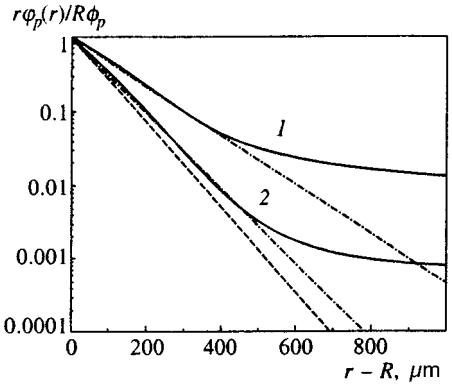

FIG. 8. Dependence of the unit-normalized product $r\varphi_p$ on distance to the surface of the particle in neon ($T_e=50000$ K, $T_i=300$ K, $N_e=5\times10^8$ cm^{-3}) for particles of radius $R=25$ μm (*1*) and $R=1.5$ μm (*2*). The dash–dot curves plot the dependence obtained from Eq. (7) with $\lambda=130$ and 85 μm, respectively. The dashed curve corresponds to Eq. (7) with $\lambda=\lambda_L$.

large interatomic distances, and a slackening of the dependence of the interparticle interaction on the electron and ion concentrations in the screening cloud.

Figure 9 plots the dependence of the screening length λ on the electron concentration N_e. Proper choice of the latter enables one to accurately approximate the calculated potential $\varphi(r)$ near the particle with the help of the Debye–Hückel potential (7). As in the case of the helium discharge,[45] at small radii it is possible to use the linear screening length λ_L, but for $R_p\sim\lambda_L$ it is necessary to allow for nonlinear effects. Note that under the conditions of interest, λ shows essentially no dependence on T_e.

Allowing for screening of the charge of the dust particles and the non-Maxwellian character of the electron and ion velocity distribution functions near the particles, as a nonideality parameter in place of Γ calculated according to Eq. (3), it is possible to use[20]

$$\Gamma_D=\frac{Z^2e^2}{aT_p}\,e^{-a/\lambda} \tag{8}$$

in the case of small Al_2O_3 particles, and

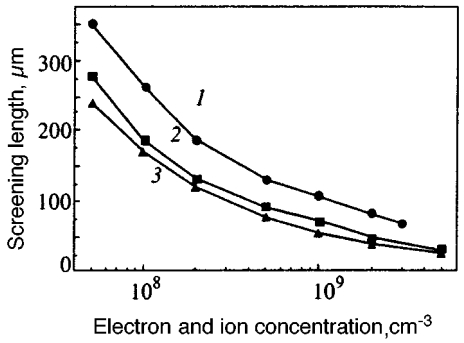

FIG. 9. Dependence of the effective screening length λ on the electron concentration N_e in neon ($T_e=50000$ K, $T_i=300$ K) for particles of radius $R=25$ μm (*1*) and $R=1.5$ μm (*2*). Curve *3* plots the linear Debye–Hückel screening length (5).

$$\Gamma_n=\frac{Z^2e^2}{aT_p}\,\frac{R_p}{2a}. \tag{9}$$

in the case of large glass particles.

In both cases, the degree of nonideality can be reduced by several orders of magnitude in comparison with Γ; however, it is still too large to explain the observed ''melting'' of the ordered structures. One reason for this is that the particles are held back not where the electrostatic force acting on them is maximum (and consequently their charge Z is also maximum), but where it balances the gravitational force. The second and probably the most important reason is that, as a consequence of the fluctuating plasma microfields, particles charged to large values of Z have mean kinetic energy T_p significantly greater than the temperature of the gas. This effect is observed both in a radio-frequency plasma[37,47] and in our experiments.[26] In both cases, with distance from the melting curve, the particle energy reaches a very high value of the order of 50 eV. Such a growth of the energy can explain the observed ''melting'' of dust crystals.

3.2. Formation of ordered structures in an electric double layer

Levitation of macroparticles in the positive column of a constant-current glow-discharge requires an electric field strong enough to balance the force of gravity and is possible not only in strata, but also in a specially organized electric double layer. Toward this end, one can vary the plasma parameters by varying the transverse cross section of the positive column.[48]

However, in contrast to Ref. 48, we use a positive column with a narrow cathode part with radius R_k and a wide anode part with radius R_a ($R_k<R_a$) with an expansion segment in between. In this case, a double layer of space charge separating the two plasma regions with different electron temperatures T_{ek} and T_{ea} and electron concentrations N_{ek} and N_{ea} appears in the mouth of the constriction. The narrow cathode part has higher values of T_{ek} and N_{ek}. The potential jump U at the double layer depends on the gas pressure, the radii R_k and R_a, their ratio R_a/R_k, and the discharge current. U can be estimated from the relation[48]

$$U=T_{ek}-T_{ea}+\frac{T_{ek}+T_{ea}}{2}\ln\frac{N_{ek}}{N_{ea}}. \tag{10}$$

Thus, for the given discharge tube the introduction of a constriction with a radius $R_k=3.5$ mm yields an increase in N_e for $p=0.5$ Torr of almost an order of magnitude, in T of a factor of three, and $U\approx10$ V. Since the longitudinal dimension of the double layer in the mouth of the constriction is not large (~1 cm), the values of the longitudinal electric field in the layer are of the same order of magnitude as at the head of the stratum. Thus, conditions are ensured for the capture and suspension of charged macroparticles, with subsequent formation of an ordered structure.

In experiments with a constriction $R_k=3.5$ mm, we did indeed obtain levitation of particles of both types in the mouth of the narrow part. The constriction was created by introducing an additional cylindrical glass tube with variable

inner diameter into the discharge tube, the wide part of which was placed over the cylindrical cathode.

3.3. Effect of dust particles on discharge parameters

At moderate pressures under stationary steady-state conditions, charge losses in a weakly ionized plasma are associated with ambipolar diffusion toward the walls of the discharge chamber.[38] In this case the electron temperature (and accordingly the longitudinal electric field) in the positive column of the glow-discharge can be determined by equating the ionization rate and the rate of ambipolar diffusion losses.

The presence of dust particles in the discharge can substantially alter this situation. The point is that for a high enough macroparticle concentration, charge loss to their surfaces becomes predominant in comparison with loss to the chamber walls. An idea of the efficiency of the two processes of charged particle loss can be had by comparing their respective rates. The rate of ambipolar losses is given by

$$\nu_d = \frac{D_a}{\Lambda^2}, \tag{11}$$

where D_a is the ambipolar diffusion coefficient, and $\Lambda = R/2.4$ is the characteristic diffusion length for cylindrical discharge geometry[38] (R is the radius of the discharge chamber). The electron loss rate to the surfaces of the dust particles in the orbital motion approximation is given by

$$\nu_p = \pi R_p^2 N_p \sqrt{\frac{8T_e}{\pi m_e}} \exp\left(\frac{e\varphi_p}{T_e}\right). \tag{12}$$

For the ambipolar diffusion coefficient the following estimate applies:[38]

$$D_a \approx D_i \frac{T_e}{T_i} \approx \frac{1}{3N_a\sigma} \sqrt{\frac{8T_i}{\pi m_i}} \frac{T_e}{T_i}. \tag{13}$$

Here σ is the resonant recharging cross section (in the case of motion of the ions in their own gas) and N_a is the atom concentration. Hence we obtain for the ratio of the characteristic rates

$$\frac{\nu_p}{\nu_d} = 3\pi R_p^2 \left(\frac{R}{2.4}\right)^2 N_p N_a \sigma \sqrt{\frac{T_i m_i}{T_e m_e}} \exp\left(\frac{e\varphi_p}{T_e}\right). \tag{14}$$

Let us estimate the macroparticle concentration for which charge loss to the particles is more probable than to the walls. Using the neon discharge parameters $N_a = 3\times 10^{16}$ cm^{-3} ($P = 1$ Torr), $T_e = 50000$ K, $T_i = 300$ K, $R_p = 30$ μm, $\sigma \approx 2\times 10^{-15}$ cm^{-2}, $e\varphi_p/T_e \approx -2$, we find from (14) that the rates coincide for $N_p \approx 250$ cm^{-3}.

Under the conditions of the experiment described here, the concentration of macroparticles of the given size was roughly an order of magnitude greater. Thus, the main channel of charge loss is probably loss to dust particles. Under such conditions, an increase in their density should be accompanied by a rise in the ionization rate needed to maintain the stationary discharge regime. This obviously means a rise in the electron temperature, and consequently the electric field, in the region in which the macroparticles are located. If this field grows to a sufficient magnitude, it will keep the particles from falling as a result of the force of gravity. This mechanism removes the quantitative disagreement between the electric field values required to compensate for the force of gravity and the electric field values usually observed at the head of the stratum in the case of heavy glass particles, and also allows a qualitative explanation of the experimentally observed suspension of an extended ordered structure of dust particles in the absence of visible stratification of the positive column of the glow discharge.

4. CONCLUSION

In the present paper we have investigated the formation of ordered structures of charged macroparticles in the positive column of a neon glow discharge. We observed the formation of quasicrystalline structures whose size and shape depended on the discharge parameters. Formation of the structures took place in a region of high electric field,which balanced the force of gravity, in standing strata and in a double electric layer created by introducing an additional cylindrical glass tube with variable inner diameter into the discharge. The effect of the discharge parameters on the possible existence of quasicrystalline dust-particle structures was investigated. It was found, in particular, that increasing the discharge current leads to the destruction of long-range order (melting of the quasicrystal).

The experiments also revealed the emergence of unusual formations of charged macroparticles. For certain values of the discharge parameters, extended filamentary structures were formed in the absence of stratification of the positive column. The length of such structures reached 6 cm. Note that this is the first reported observation of such structures.

The electrostatic interaction between dust particles, which leads to the formation of ordered structures, was considered in detail with allowance for the nonlinearity of screening with a non-Maxwellian energy distribution of the electrons and ions of the plasma. A difference in the shape of the interaction potential is noted for different sorts of macroparticles (due to a difference in their diameters). An estimate was made of the coupling parameter Γ corresponding to the existence of ordered structures. We point out the necessity of allowing for an additional channel of electron and ion loss in the presence of high dust-particle concentration in the discharge.

ACKNOWLEDGMENTS

We thank Yu. B. Golubovskiĭ, L. D. Tsendin, and V. V. Zhakhovskiĭ for useful discussions. This work was carried out with the partial financial support of the Russian Fund for Fundamental Research (Grant No. 97-02-17565) and a joint grant from the Russian Fund for Fundamental Research and INTAS (Grant No. 95-1335).

*)E-mail: Nefedov@hedric.msk.su

[1] I. Langmuir, G. Found, and A. F. Dittmer, Science **60**, 392 (1924).
[2] S. L. Soo, *Multiphase Fluid Dynamics*, Gower Technical, Brookfield, Vermont (1990).
[3] M. S. Sodha and S. Guha, Adv. Plasma Phys. **4**, 219 (1971).
[4] D. I. Zhukhovitskiĭ, A. G. Khrapak, and I. T. Yakubov, in *Plasma Chemistry*, B. M. Smirnov (ed.), **11**, 130 (1984).

[5] I. T. Yakubov and A. G. Khrapak, Sov. Tech. Rev. B: Thermal Phys. **2**, 269 (1989).
[6] B. M. Smirnov, *Aerosols in Gas and Plasma* [in Russian], IVTAN Press, Moscow (1990).
[7] C. K. Goetz, Rev. Geophys. **27**, 271 (1989).
[8] T. G. Northrop, Phys. Scr. **45**, 475 (1992).
[9] V. N. Tsytovich, Usp. Fiz. Nauk **167**, 57 (1997).
[10] A. Garscadden, B. N. Ganguly, P. D. Haaland, and J. Williams, Plasma Sources Sci. Technol. **3**, 239 (1994).
[11] A. Bouchoule and L. Boufendi, Plasma Sources Sci. Technol. **3**, 292 (1994).
[12] J. Goree, Plasma Sources Sci. Technol. **3**, 400 (1994).
[13] G. S. Selwyn, in *The Physics of Dusty Plasmas*, P. K. Shukla, D. A. Mendis, and V. W. Chow (eds.), World Scientific, Singapore (1996), p. 177.
[14] Yu. P. Raĭzer, M. N. Shneĭder, and N. A. Yatsenko, *High-Frequency Capacitive Discharge* [in Russian], MFTI Press and Nauka, Moscow (1995).
[15] J. E. Allen, Phys. Scr. **45**, 497 (1992).
[16] S. Ichimaru, Rev. Mod. Phys. **54**, 1017 (1982).
[17] V. E. Fortov and I. T. Yakubov, *Nonideal Plasma* [in Russian], Énergoatomizdat, Moscow (1994).
[18] V. E. Fortov, A. P. Nefedov, O. F. Petrov, A. A. Samarian, A. V. Chernyschev, and A. M. Lipaev, JETP Lett. **63**, 187 (1996).
[19] V. E. Fortov, A. P. Nefedov, O. F. Petrov, A. A. Samarian, and A. V. Chernyschev, Phys. Lett. A **219**, 89 (1996).
[20] H. Ikezi, Phys. Fluids **29**, 1764 (1986).
[21] J. H. Chu and L. I, Phys. Rev. Lett. **73**, 652 (1994).
[22] H. Thomas, G. E. Morfill, V. Demmel *et al.*, Phys. Rev. Lett. **73**, 652 (1994).
[23] A. Melzer, T. Trottenberg, and A. Piel, Phys. Lett. A **191**, 301 (1994).
[24] Y. Hayashi and K. Tachibana, Jpn. J. Appl. Phys., Part 2 **33**, L804 (1994).
[25] V. E. Fortov, A. P. Nefedov, V. M. Torchinskiĭ, V. I. Molotkov, A. G. Khrapak, O. F. Petrov, and K. F. Volykhin, JETP Lett. **64**, 92 (1996).
[26] V. E. Fortov, A. P. Nefedov, V. M. Torchinsky, V. I. Molotkov, O. F. Petrov, A. A. Samarian, A. M. Lipaev, and A. G. Khrapak, Phys. Lett. A **229**, 317 (1997).
[27] E. Wigner, Phys. Rev. **46**, 1002 (1934).
[28] H. Jiang, R. L. Willet, H. Stormer *et al.*, Phys. Rev. Lett. **65**, 633 (1990).
[29] R. F. Wuerker, H. Shelton, and R. V. Langmuir, J. Appl. Phys. **30**, 342 (1959).
[30] F. Diedrich, E. Peik, J. M. Chen *et al.*, Phys. Rev. Lett. **59**, 2931 (1987).
[31] S. L. Gilbert, J. J. Bollinger, and D. J. Wineland, Phys. Rev. Lett. **60**, 2022 (1988).
[32] I. Waki, S. Kassner, G. Birkl, and H. Walther, Phys. Rev. Lett. **68**, 2007 (1992).
[33] A. K. Sood, Solid State Phys. **45**, 1 (1991).
[34] B. Deryagin and L. Landau, Acta Phys. Chim. USSR **14**, 633 (1941).
[35] F. M. Kuni, *Statistical Physics and Thermodynamics* [in Russian], Nauka, Moscow (1981).
[36] T. Hill, *Statistical Mechanics: Principles and Selected Applications*, McGraw-Hill, New York (1956).
[37] H. M. Thomas and G. E. Morfill, Nature (London) **379**, 806 (1996).
[38] Yu. P. Raĭzer, *Gas-Discharge Physics* [in Russian], Nauka, Moscow (1987).
[39] Yu. P. Raĭzer, *Principles of the Contemporary Physics of Gas-Discharge Processes* [in Russian], Nauka, Moscow (1980).
[40] Yu. B. Golubovskiĭ, S. U. Nisimov, and I. É. Suleĭmenov, Zh. Tekh. Fiz. **64**, 54 (1994) [Tech. Phys. **39**, 1005 (1994)].
[41] Yu. B. Golubovskiĭ and S. U. Nisimov, Zh. Tekh. Fiz. **65**, 46 (1995) [Tech. Phys. **40**, p. (1995)].
[42] Yu. B. Golubovskiĭ and S. U. Nisimov, Zh. Tekh. Fiz. **66**, 20 (1996) [Tech. Phys. **41**, p. (1996)].
[43] P. S. Landa, N. A. Miskinova, and Yu. V. Ponomarev, Usp. Fiz. Nauk **132**, 601 (1980) [Sov. Phys. Usp. **23**, 813 (1980)].
[44] L. D. Tsendin, Fiz. Plazmy **8**, 400 (1982) [Sov. J. Plasma Phys. **8**, 228 (1982)].
[45] J. E. Daugherty, R. K. Porteous, and D. B. Graves, J. Appl. Phys. **73**, 1617 (1993).
[46] J. E. Daugherty, R. K. Porteous, M. D. Kilgore, and D. B. Graves, J. Appl. Phys. **72**, 3934 (1992).
[47] A. Melzer, A. Homann, and A. Piel, Phys. Rev. E **53**, 2757 (1996).
[48] V. L. Granovskiĭ, *Electrical Current in a Gas. Steady-State Current* [in Russian], Nauka, Moscow (1971).

Translated by Paul F. Schippnick